

# GEOCHEMICAL EVALUATION OF THE LATE MAASTRICHTIAN SUBDUCTION-RELATED VOLCANISM IN THE SOUTHERN NEOTETHYS IN VAN AREA, AND A CORRELATION ACROSS THE TURKISH-IRANIAN BORDER

**Ali Rıza Çolakoğlu\***, **Kurtuluş Günay\*\***, **M. Cemal Göncüoğlu\*\*\*,✉**, **Vural Oyan°** and **Kemal Erdoğan\*\***

\* *Geological Engineering Department, Yüzüncü Yıl University, Van, Turkey*

\*\* *General Directorate of Mineral Research and Exploration, Kocaeli, Turkey*

\*\*\* *Geological Engineering Department, Middle East Technical University, Ankara, Turkey.*

° *Mining Engineering Department, Yüzüncü Yıl University, Van, Turkey*

✉ *Corresponding author, e mail: mcgoncu@metu.edu.tr*

**Keywords:** *Yüksekova mélange, late Maastrichtian, N branch of southern Neotethys, back-arc basalt, Turkish-Iranian border.*

## ABSTRACT

The Yüksekova mélange to the NE of Van, close to the Turkish-Iranian border is part of the Berit-Elazığ-Van ophiolitic belt. It structurally overlies the Bitlis-Pütürge metamorphic complex and includes the remnants of the southern Neotethys. The mélange complex comprises mantle rocks together with massive and pillowed lavas and dykes associated with late Maastrichtian micritic limestones and radiolarian cherts. The lavas are trachyandesite/basaltic, whereas the dykes are alkali basalt in composition. Both rock types were probably formed by low-degree partial melting of a mixed source including primitive mantle and depleted MOR mantle components, which were subsequently affected by subduction modification. The geochemical character constrains the formation of these basalts, yet the youngest ones dated in the Yüksekova mélange to an intra-oceanic subduction zone within the Neotethys at the end of Cretaceous. The new ages and the tectonic setting of the volcanic rocks are correlated with other oceanic assemblages (e.g., Khoy and Inner Zagros ophiolites in Iran) across the Turkish-Iranian border.

## INTRODUCTION

Remnants of the Tethyan oceanic lithosphere are found in Turkey mainly as dismembered ophiolitic bodies within accretionary mélangé complexes. These mélangé complexes either crop out in their original position, marking the sutures, or as allochthonous bodies. They may also arise as dismembered bodies or as olistoliths in peripheral fore-deep basins. In the eastern Mediterranean, the remnants of the southern branch of the Neotethys Ocean follow a continuous belt (the peri-Arabian ophiolite belt) from Cyprus to the Amanos Mountains on the eastern Mediterranean coast, the Turkish-Iranian border, along the Zagros suture belt to Oman and Makran (Fig. 1). In the SE Anatolian area the location of this suture was a matter of debate (see e.g., Robertson, 2006; 2007). Şengör et al. (1979) initially suggested the name Bitlis Suture for this main structure between the Tauride-Anatolide micro-continent and the Arabian Autochthon. Then (Şengör, 1984), it was separated in three different suture belts (Assyride, Çüngüş and Maden sutures). The same was named as the Amanos-Elazığ-Van suture belt by Göncüoğlu et al. (1997), who located it to the N of the Pütürge-Bitlis massifs. In the last years, however, it is commonly accepted (e.g., Oberhaensli et al., 2012; Parlak et al., 2012; Karaoğlu et al., 2013; 2014) that it actually consists of two parallel belts. The southern belt with ophiolitic bodies and mélangé complexes (e.g., Kızıldağ, Baer-Bassit, Gaziantep, Koçali and Cilo ophiolites) is located to the south of the Pütürge-Bitlis massifs (Fig. 1), where oceanic assemblages are emplaced onto the non-metamorphic platform and fore-deep sediments of the N Arabian margin (Yılmaz, 1985; Varol et al., 2011). Towards east, it continues in

Iran along the Sanandaj-Sirjan metamorphic massifs. The northerly located basin, also known as the Berit Ocean (e.g., Robertson et al., 2012; 2013) representing the remnants of the Berit-Elazığ-Van ophiolitic belt (Göncüoğlu, 2010), is bounded in the north by Paleozoic-Mesozoic platformal rocks of the Tauride-Anatolide Terrane and in the south by the Pütürge-Bitlis massifs (Göncüoğlu and Turhan, 1984) representing the metamorphic northern edge of the Arabian plate.

The geological features and the tectono-magmatic setting of the ophiolitic rocks in the western part of the Berit-Elazığ-Van ophiolitic belt was relatively well-studied (e.g., Robertson, 2002; Bağcı et al., 2005; Dilek and Thy, 2009; Parlak et al., 2009). However, the eastern part of this belt between Elazığ and the Turkish-Iranian border is less-known, as it is buried under the Miocene-Quaternary volcanic rocks. Şengör et al. (2003) considers this area as a huge mélangé prism (the East Anatolian Accretional Prism (EAAC)). Based upon the presence of some low grade metamorphic massifs, other authors (e.g., Göncüoğlu et al., 1997; Yılmaz et al., 2014), suggest that the Tauride-Anatolide platform continues beneath the volcanic cover towards Iran and separates the suture of the southern Neotethys from the northerly located Izmir-Ankara-Erzincan-Alborz branch of Neotethys (Fig. 1).

Moreover, in contrast to the western part of the Berit-Elazığ-Van ophiolitic belt, the geochemical character and age of the oceanic lithosphere in the segment between Elazığ and the Turkish-Iranian border (Fig. 1) is poorly constrained (e.g., Çolakoğlu et al., 2012). The scarcity of the data has resulted in a number of conflicting models on the geodynamic evolution of the southern Neotethyan branch

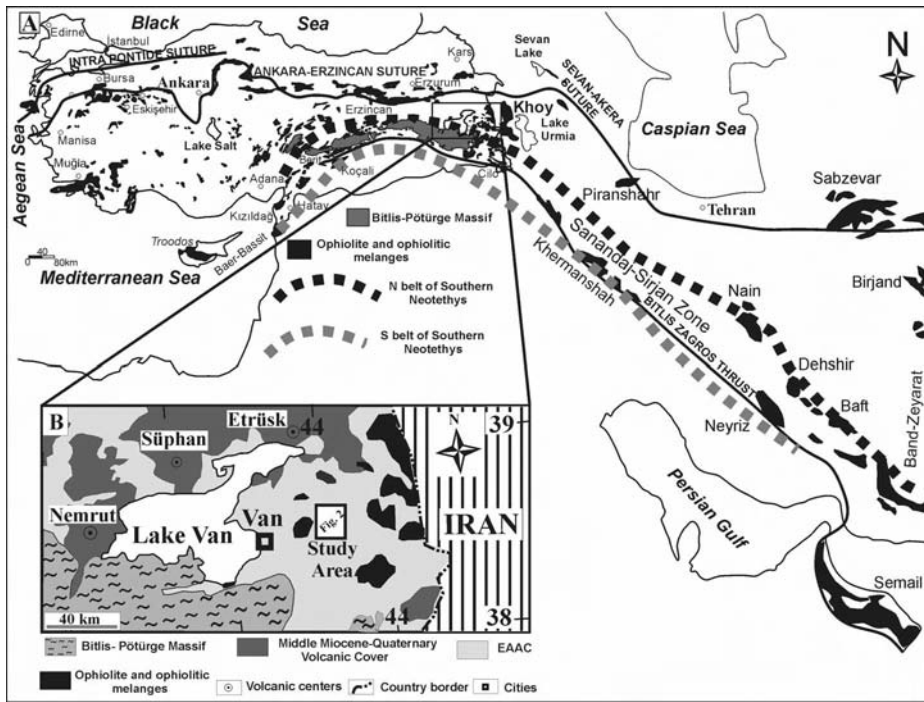


Fig. 1 - (A) Distribution of ophiolites, ophiolitic mélanges and ophiolitic belts from southern Turkey to Iran; (B) location of the study area in Eastern Anatolia.

(for details see Robertson, 2006). A critical constraint of these models is the age of the intra-oceanic decoupling that resulted in the closure of this ocean. One group of authors suggests that this ocean had not closed prior to the end of Paleogene (Şengör and Yılmaz, 1981; Dilek et al., 2010), whereas others (Göncüoğlu et al., 1997; Rolland et al., 2011; Çolakoğlu et al., 2012) suggest a latest Cretaceous initial closure, followed by emplacement of oceanic and variably-metamorphosed platform-margin units onto the metamorphosed northern edge of the Arabian Platform. Both suggestions are speculative and not supported by reliable data. Another critical issue regards the continuation of the suture belt towards east into NE Irak and S Iran as seen in several regional maps showing the location of the Tethyan sutures (see e.g., Blome and Irwin, 1985; Robertson, 2006; Dilek et al., 2010).

This paper presents new geochemical data on the ophiolitic pillow basalts within Yüksekova mélangé to the north of the Bitlis Massif together with paleontological data from the associated intra-pillow micritic limestones. Although the data has been derived from a small ophiolitic body, they represent the first reliable data on the age of intra-oceanic subduction from the eastern part of the southern Neotethys in the eastern part of the Berit-Elazığ-Van ophiolitic belt in southeastern Turkey.

## GEOLOGICAL FRAMEWORK

In the east of Lake Van (Fig. 1A, B), tectonic slices of metamorphic rocks, of an ophiolitic mélangé (Yüksekova mélangé) and Paleogene flysch sediments with olistoliths (Ketin, 1977; Acarlar et al., 1991; Elmas, 1992; Şenel and Ercan, 2002; Şengör et al., 2008) crop out underneath a thick cover of Neogene and Quaternary volcanic and volcanoclastic rocks. The Yüksekova mélangé comprises lithologies of a dismembered ophiolitic succession, an island arc and oceanic sediments (Perinçek, 1990; Yılmaz, 1993; Elmas and Yılmaz, 2003). The available biostrati-

graphic data from the overlying flysch sediments (Seske Formation) range from Middle Paleocene to Eocene (Şenel et al., 1984). Both formations are covered by the Pliocene-Pleistocene Saray formation and recent alluviums.

## Geology of Study Area

The Yüksekova mélangé in the studied area (Fig. 2A) has been recently mapped at scale of 1:10.000. It comprises two distinct tectonic units. The first unit at the center of the map area consists of massive and pillow lavas intercalated with reddish, pelagic, fossiliferous limestones, mudstones, and radiolarian cherts. The radiolarian cherts occur as small bands within both basalts and pelagic limestones. These volcanic and volcano-sedimentary units are bounded to the south by splays of the east-west trending Özalp Active Fault (Figs. 2A, B, 3A, B).

The micritic rocks fill the intra-pillow spaces and include hyaloclastic clasts near the contact with the pillow lavas (Fig. 3C, D, E). The pillow lava lobes in contact with these sediments show chilled margins, and the pink micritic limestones at their contacts have a thin contact zone of fine grained and brick red recrystallized limestone with sugary texture. The occurrence of angular basaltic fragments (Fig. 3F, G) within the micritic limestone-chert deposits, together with patches of micritic limestones within basalts indicates that the basaltic extrusions were contemporaneous with the deposition of lime mud near the carbonate compensation depth in a deep oceanic basin. The entire volcano-sedimentary assemblage is intruded by dykes of lamprophyric nature (Fig. 3H).

The micritic limestones are rich in foraminifers. From these limestones we obtained (Fig. 4): *Racewiguembelina fructicosa* (Egger), *Racewiguembelina fructicosa* (Egger), *Contusotruncana contusa* (Cushman), *Globotruncanita stuarti* (De Lapparent), *Globotruncanella havanensis* (Voorwijk) and *Globotruncanella contusa* (Cushman). This assemblage is indicative of a late Maastrichtian depositional age of the micritic sediments and concomitant volcanism.

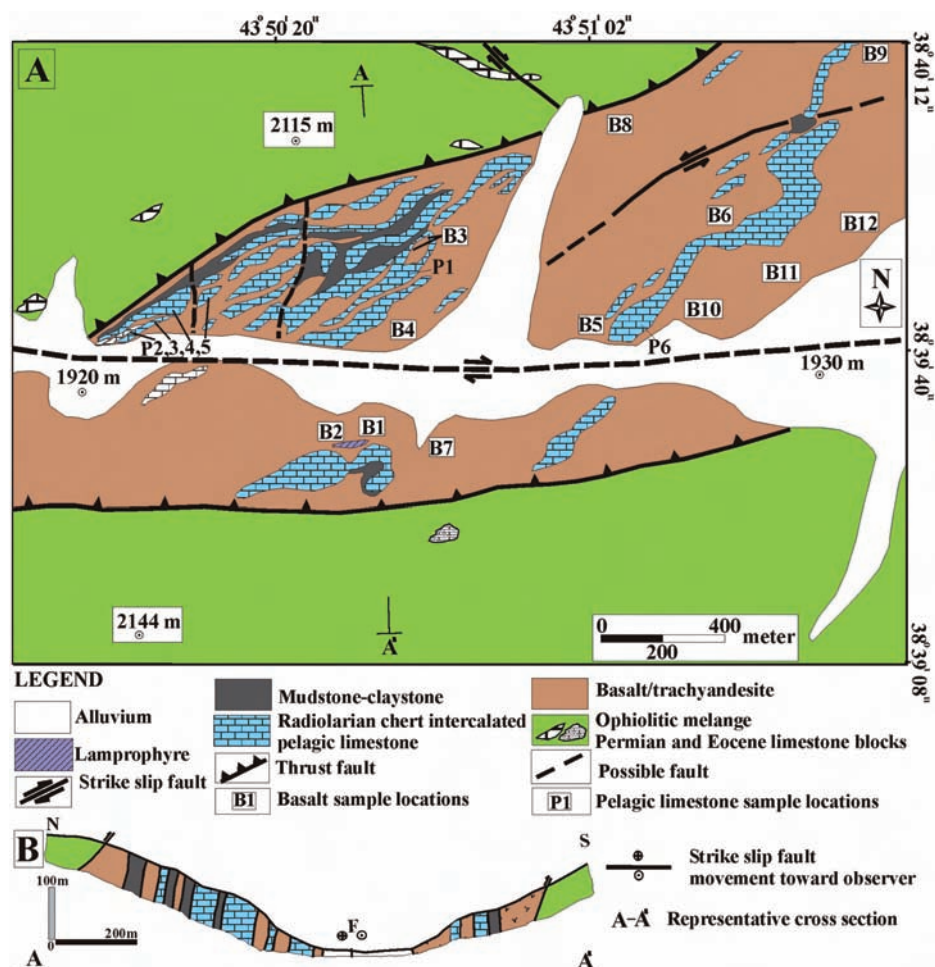


Fig. 2 - (A) geological map of the study area also showing the sample locations and (B) generalized cross section of the studied units.

The second structural unit crops out to the north and south of the volcanic unit and structurally overlies the lavas. It is a sedimentary mélangé consisting of olistoliths of peridotites, gabbros, serpentinites, plagiogranites, fossiliferous Paleocene and Permian limestones within a deformed matrix of shales, sandstones and olistostromal conglomerates.

Highly deformed Eocene olistostromal sediments rest by angular unconformity on the slices and olistoliths of the Yüsekova mélangé and the Late Cretaceous flysch sediments.

### Petrography

The volcanic rocks have undergone low grade metamorphism and alteration. The mafic lavas and dikes are petrographically trachyandesite/basaltic and alkali basalts respectively.

Basalts have intersertal and doleritic textures and are modally dominated by plagioclase (with  $An >_{60}$ ) microlites and phenocrysts (Fig. 5A, B) in a groundmass of partly devitrified volcanic glass. Carbonatization, chloritization and sericitization of plagioclase and chloritization of glass are common alteration products. Doleritic basalts are medium-grained rocks formed principally of plagioclase laths (labradorite) with an average grain size of 200-500  $\mu\text{m}$ . The groundmass includes uralitized augite and iddingsitized olivine.

The dykes display porphyritic texture and are formed principally by phenocrysts of titanite (35%) and barkeite (30%). These minerals are fresh, euhedral and zoned

with a grain size between 1 and 4 mm. The matrix contains fine-grained (10-100  $\mu\text{m}$ ) titanite (15%), barkeite (13%), olivine (3%), apatite (2%) and plagioclase (2%) (Fig. 5C, D). Olivine (50-300  $\mu\text{m}$ ) has been generally transformed into iddingsite and magnetite. The apatite is fresh and euhedral while the microlites of plagioclase have been replaced by sericite.

### ANALYTICAL METHODS

Two relatively fresh basaltic dykes and seven pillow lava samples were chosen for geochemical analyses. Major oxide, trace and rare earth element concentrations were determined at the ALS Chemex Analytical Laboratories in Toronto - Canada. A 0.9 g sample is added to 9.0 g of Lithium Borate Flux (50%  $\text{Li}_2\text{B}_4\text{O}_7$  - 50%  $\text{LiBO}_2$ ), mixed well and fused in an automatic furnace to between 1050-1100°C. The major elements were quantified as oxides using X-ray fluorescence spectroscopy on the fused sample.

Inductively Coupled Plasma-Mass Spectrometry (ICP-MS) was used to determine trace and rare earth elements. A grinded sample (0.200 g) is added to lithium metaborate flux (0.90 g), mixed well and fused in a furnace at 1000°C. The resulting melt is then cooled and dissolved in 100 mL of 4%  $\text{HNO}_3$  / 2%  $\text{HCl}$  solution. The resulting solution is then analyzed by inductively coupled plasma-mass spectrometry. Quality control limits for reference materials and duplicate analyses are established according to the precision and accuracy requirements of the particular method.

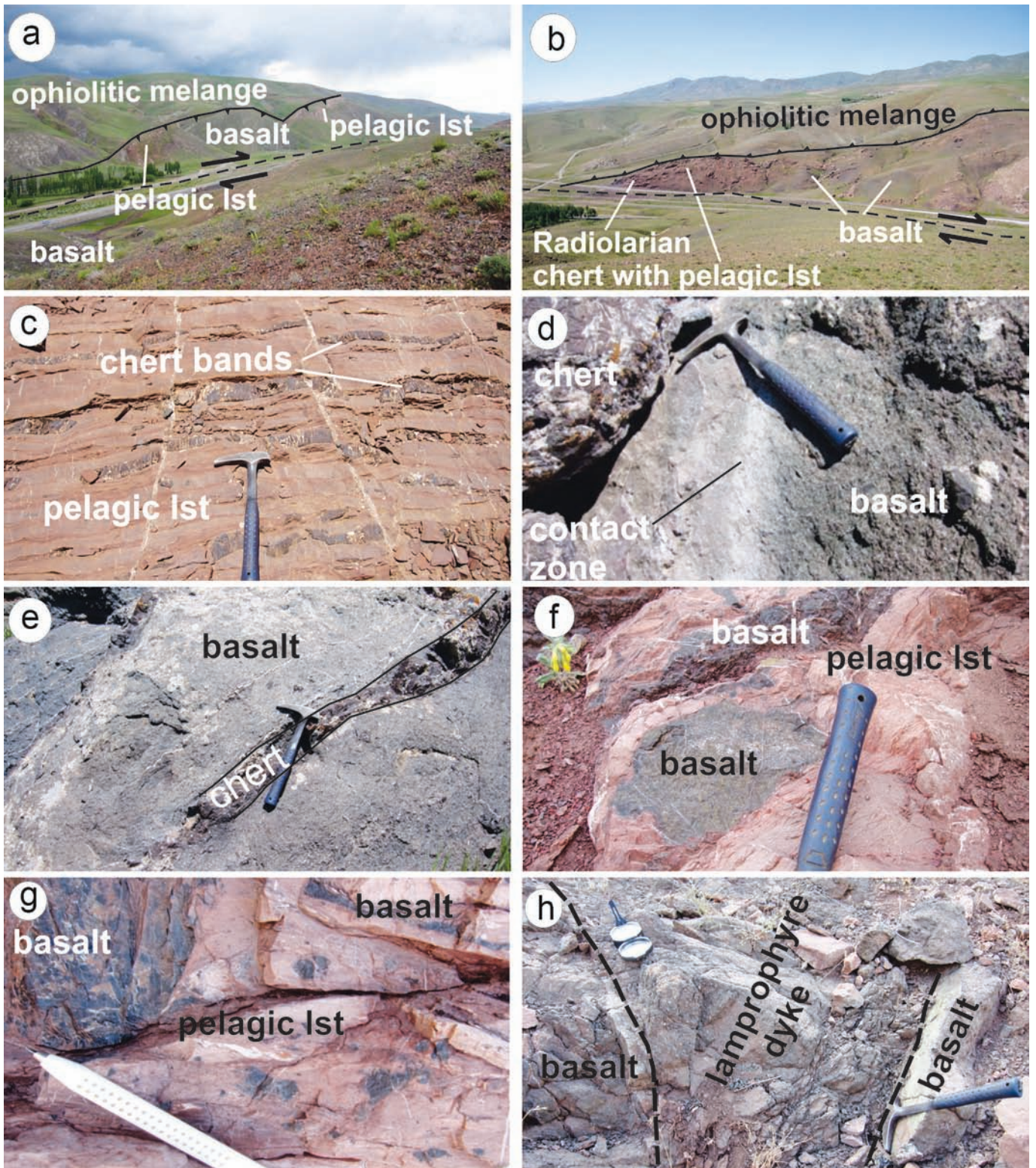


Fig. 3 - Field photos of the volcanic rocks, the mélangé sediments and their structural relationships (a and b), view of ophiolitic mélangé structurally overlying basalt - pelagic limestones (1<sup>st</sup>) unit along a thrust contact, (c) radiolarian cherts intercalated with pelagic limestones showing (d-e) a chert band between two pillow-lava lobes (f) angular fragment of basalt within synsedimentary chert-micritic limestones. (g) basalt clasts in the pelagic limestone, (h) porphyritic dyke cutting the aphyric textured basalt.

### GEOCHEMISTRY

The data obtained as a result of these analyses indicate that loss-on-ignition (LOI) values of the studied samples varies between 4 and 8 wt% and that they might have been affected

by hydrothermal alteration, low grade metamorphism and sea floor alteration. The results are reported in Table 1. Some major and trace elements, especially the large ion lithophile elements (LILE) ones are susceptible to remobilization under hydrothermal alteration or low grade metamorphic conditions

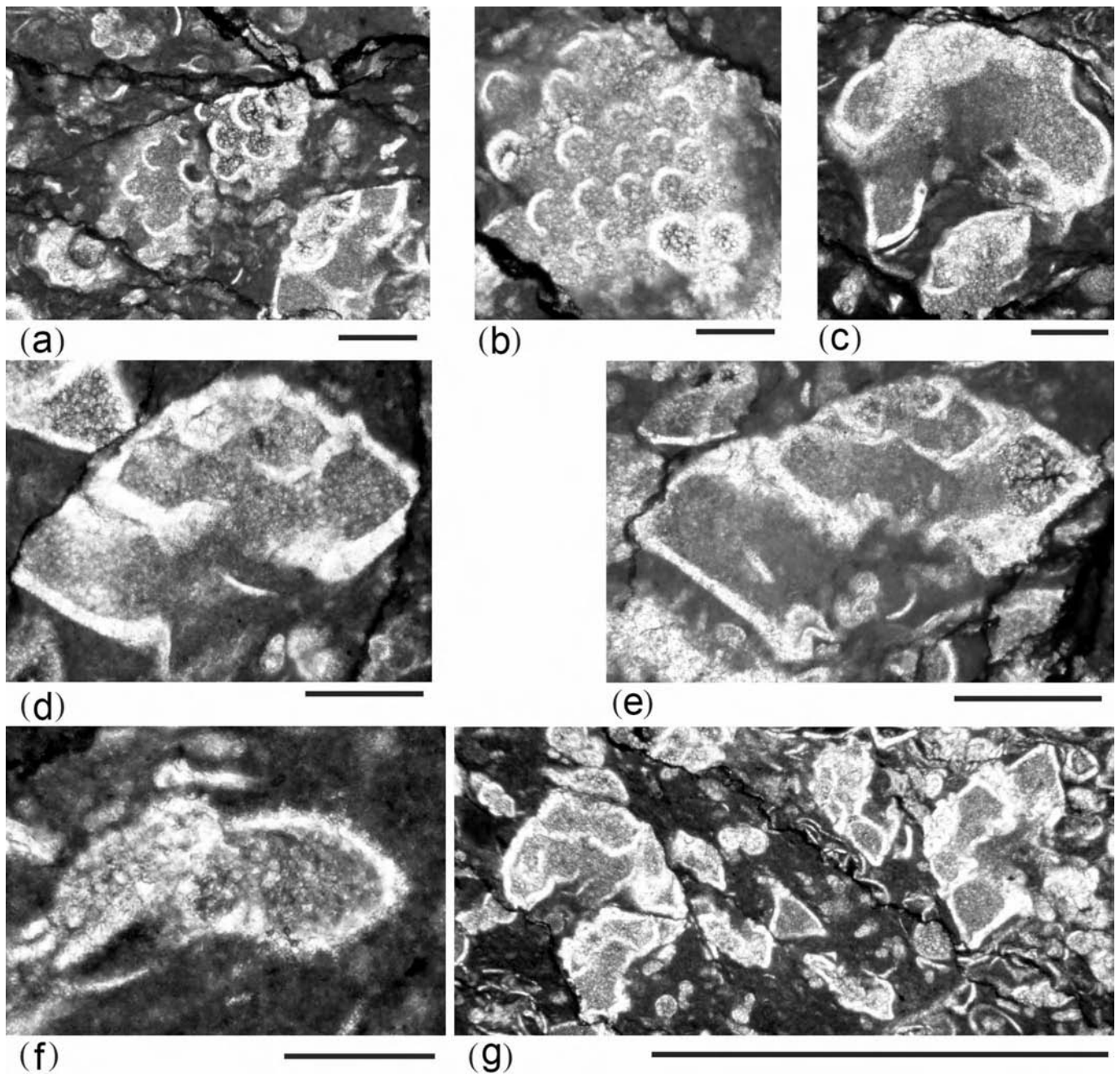


Fig. 4 - Late Maastrichtian fossils in pelagic limestone samples: (a) *Racewiguembelina fructicosa* (Egger); (b) *R. fructicosa* (Egger); (c) *Contusotruncana contusa* (Cushman); (d) *Globotruncanita stuarti* (De Lapparent); (e) and *G. stuarti* (De Lapparent); (f) *Globotruncanella havanensis* (Voorwijkstra); (g) *G. contusa* (Cushman) and *Globotruncanita stuarti* (De Lapparent). Scale bar: 0.25 mm.

(e.g., Wood et al., 1976; Floyd and Winchester, 1978; McLean and Barret, 1993; Bienvenu et al., 1990). However, the concentration or ratios of high field-strength elements (HFSE) such as Y, Zr, Nb, Ta, Ti and the rare earth elements (REE) are known to be less-mobile (Pearce and Cann, 1973; Floyd and Winchester, 1978). Thus, geochemical characteristics and petrogenetic interpretations of dyke and lava samples are based on REE and HFSE geochemistry.

Nb/Y vs Zr/TiO<sub>2</sub> variation diagrams (Winchester and Floy, 1977) have been used to classify the studied rocks. The samples cluster in the alkali-basalt, basanite and trachyandesite fields (Fig. 6). While the SiO<sub>2</sub> content of the dyke and lava samples varies between 41 and 48 wt%, trachyandesite samples have higher SiO<sub>2</sub> contents (47-53 wt%) than basaltic

samples. High Mg numbers ( $100 \times \text{Mg}^{2+} / (\text{Mg}^{2+} + \text{Fe}^{2+})$ ) between 55 and 68 of the dyke and lava samples indicate that they are of primary magmatic composition. Conversely, relatively low Mg number values (39-65) of trachyandesite samples could be the result of fractional crystallization processes. Dykes are mostly silica-undersaturated (normative nepheline ~ 10%) and have higher MgO contents with respect to lava samples.

TiO<sub>2</sub> concentration of the basaltic samples range from 0.98 to 1.71 wt%, indicating mixing of different mantle compositions and (or) low partial melting degree. In addition, the trachyandesite samples have lower TiO<sub>2</sub> content than basalts. This may be associated with fractionation of oxide minerals.



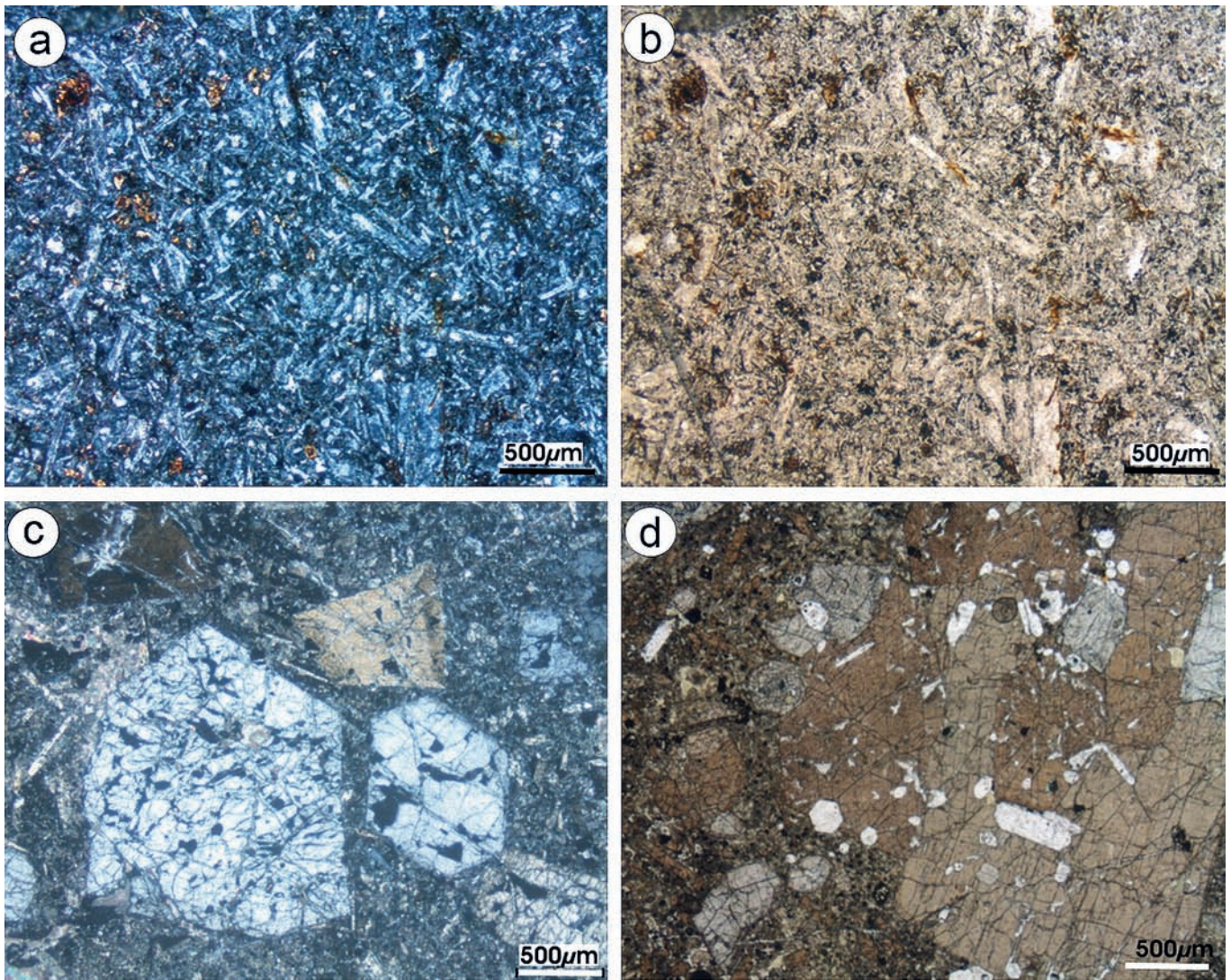


Fig. 5 - Microphotographs of lava (a-b) and dyke samples (c-d). (a) Doleritic basalt with laths of plagioclase. The gaps are filled by fine grained plagioclase, uralitized augite and iddingsitized olivine (left corner and centre) (a) cross polarized light and (b) plain polarized light); (c) Euhedral phenocrysts of titanaugite (larger phenocryst) and barkevikite (central and right) within a matrix of titanaugites and barkevikites, plagioclases and apatites (polarized light); (d) Poikilitic titanaugite and barkevikite (brown) with several apatite (white) inclusions (plain polarized light).

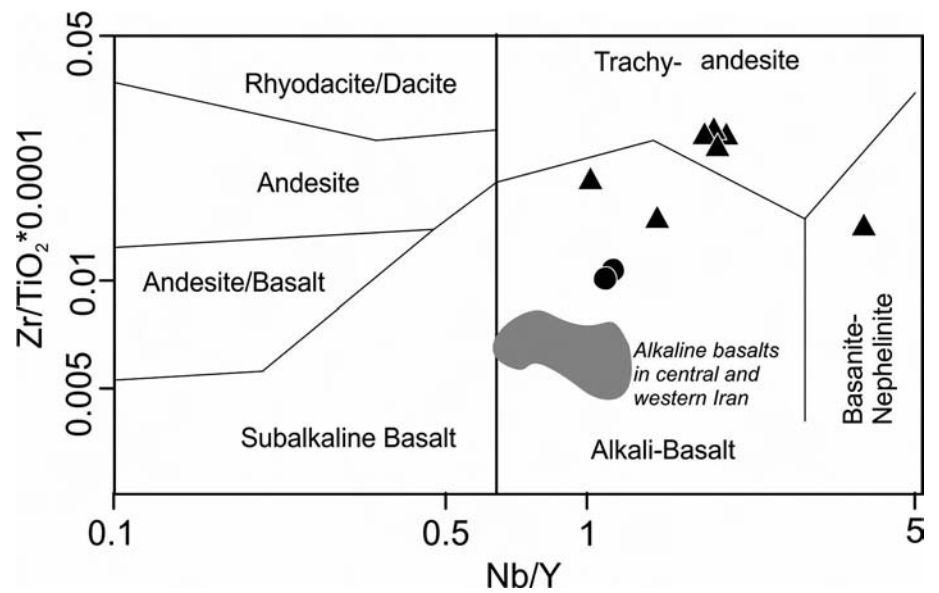


Fig. 6 - Distribution of the studied samples on Zr/TiO<sub>2</sub> vs Nb/Y classification diagrams of Winchester and Floyd (1977). For the geochemical data from Iran see text.

On the Nb-Zr-Y ternary diagram (Meschede, 1986) basic lava and dyke samples plot in within plate basalts (WPB) and within plate tholeiites (Fig. 7a) fields. In Zr/Y vs Zr discrimination diagrams (Fig. 7b) the samples plot in the within plate basalt (WPB) field. The trachyandesites exhibit a trend towards outside this field with increasing Zr/Y values.

Fig. 8a and c display N-MORB-normalized multi-element patterns of the dykes and lavas, respectively. In these diagrams, typical ocean island basalt (OIB) patterns are plotted for comparison. All samples display enrichment in LILE, high field-strength elements (HFSE) and light-middle rare earth elements (L-REE and MREE respectively). Limited depletion in heavy rare earth elements (HREE) relative to normal mid-ocean ridge basalts (N-MORB) composition is also evident. Although the trends of the samples are similar to typical OIB (or within plate basalts), note that all samples display slightly negative anomalies of HFSE (such as Ta, Nb, Zr, Hf, Ti) with respect to adjacent LILE (Th) and REE. Conversely, the irregular LILE pattern of the lava samples (Fig. 8c) arises from hydrothermal alteration.

The REE pattern of the samples is shown in Fig. 8b and d. In addition, the patterns of typical OIB and MORB are shown on the diagrams. As can be seen in Fig. 8b and d, all samples display enrichment of LREE relative to HREE ( $La/Yb_N = 19-25$ , where the subscript N denotes normalization to chondrite). Although the patterns of the samples are similar to typical OIB, they have higher LREE concentration with respect to OIB.

## DISCUSSION

### Source characteristics

OIB and MORB generally exhibit positive Nb-Ta-Ti anomalies and negative Pb anomalies in N-MORB or primitive mantle-normalized multi-element diagrams (e.g., Hofmann, 1986; 1988; 1997). In contrast, all studied sam-

ples display slightly negative Nb-Ta-Ti anomalies and positive Pb anomalies with respect to LILE and REE, indicating that they were not derived from N-MORB and (or) OIB source mantle. These observations imply that dyke and lava samples could have been derived from mixing of different sources rather than directly from a normal asthenospheric source.

Experimental data (Brenan et al., 1995; Keppler, 1996) and geochemical-isotopic studies (Pearce and Parkinson, 1993; Hawkesworth et al., 1993; 1997; Pearce and Peate, 1994; Turner et al., 2003; Pearce et al., 2005) show that magmatic rocks in arc settings related to subduction of oceanic lithosphere are characterized by enrichment in LILE with respect to HFSEs and MREE to LREEs, with negative Nb, Ta, Ti anomalies and positive Pb anomalies relative to adjacent LILE (Th) and REE in N-MORB and primitive mantle-normalized multi-trace element diagrams. Multi-trace element patterns (Fig. 8A, C) of the studied rocks display negative Nb, Ta, Ti and positive Pb anomalies relative to adjacent elements and this indicates that all the samples could be derived from a mantle source enriched by a subduction component. In addition, HREE fractionation with respect to LREE observed in all samples implies that garnet may have been the residual phase in their mantle source, as partition coefficients for HREE in garnet are high ( $D_{HREE}^{Garnet-melt} \sim 2-5.5$ ; Irving and Frey, 1978; McKenzie and O'Nions, 1991; Adam and Green, 2006) and (or) they may have been formed from a small degree of partial melting.

Th/Yb values for all samples have been plotted against their Ta/Yb values in order to determine the processes in the mantle source region. Ta and Th are highly incompatible in mafic to intermediate melts and behave similarly during melting and fractional crystallization processes. Yb is incompatible and used as the normalizing factor to minimize the effects of assimilation, fractional crystallization and crystal accumulation (Keskin et al., 1998; Aldanmaz et al., 2006). Thus,  $(Ta/Yb)/(Th/Yb)$  ratios are independent of the

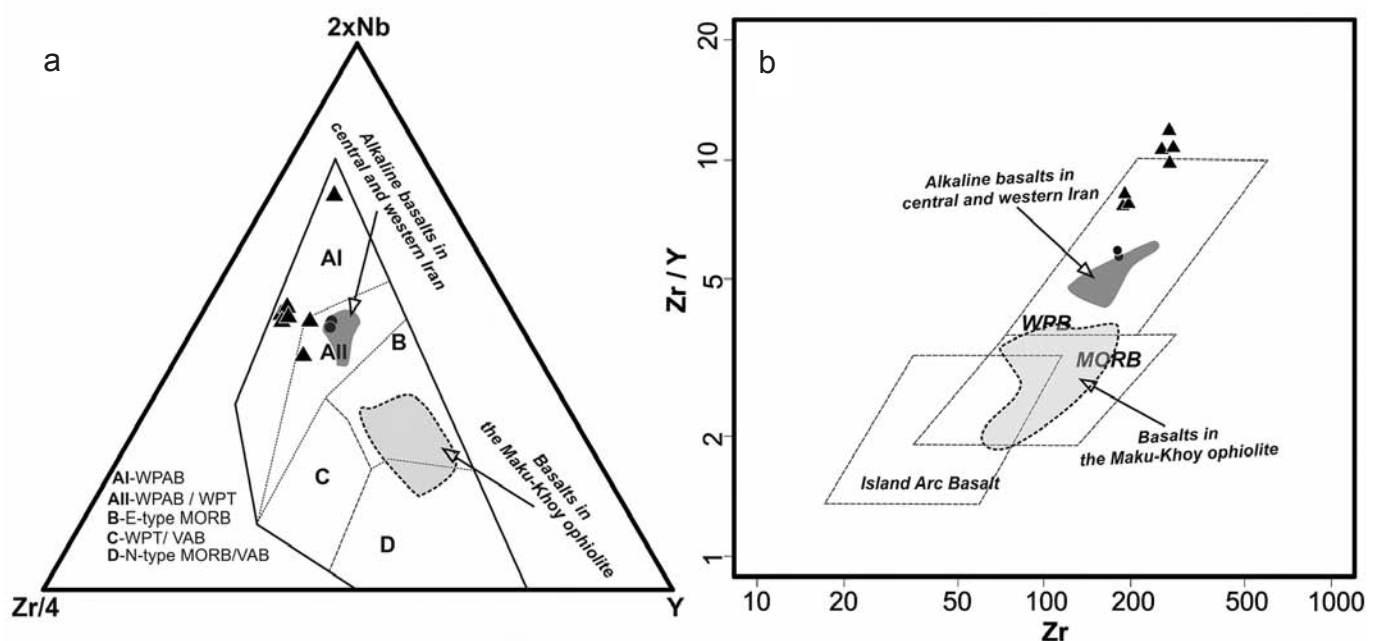


Fig. 7 - (a) Nb-Zr-Y ternary (after Meschede, 1986) and (b) Zr-Zr/Y discrimination diagrams (Pearce and Norry, 1979) for dyke and lava samples. For the geochemical data from Iran see text.

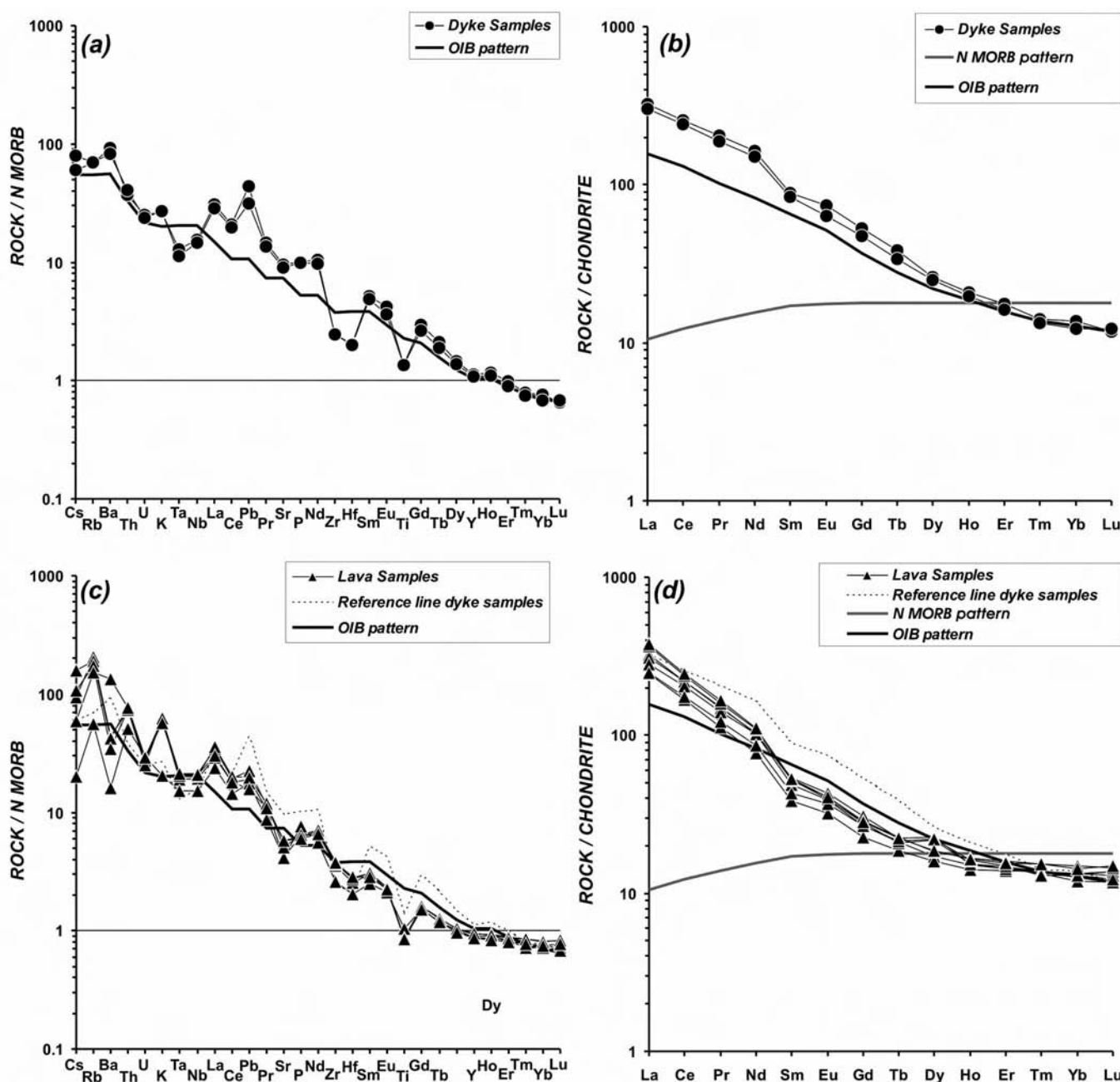


Fig. 8 - N-MORB-normalized incompatible elements (a, c) and Chondrite-normalized REE patterns (b, d) for the studied rocks (normalizing values are from Sun and McDonough (1989)).

effects of fractional crystallization and partial melting. Basalts derived from convecting upper mantle, plume asthenosphere and lithosphere are enriched by small degree partial melts from the convecting upper mantle plots within or close to mantle array, as defined by constant Th/Ta ratios in this diagram, because of similar behaviour of the Ta and Th. However, source regions enriched by a subduction component contain higher Th ratios relative to Ta and this corresponds to displacement from the mantle array with rising Th/Yb values. In the Ta/Yb vs Th/Yb diagram (Fig. 9A) all of the samples plot close to OIB field within the mantle array but they display less deviation from the mantle array towards higher Th/Yb ratios. This indicates that the samples may have been derived from mixing between an OIB-like source and a source less enriched by a subduction component. This deviation may also be due to crustal contamina-

tion but low La/Nb ratios (between 1.65-2.7) from the most primitive samples imply that they have not been affected or point out for minimal crustal contamination as low La/Nb ratios ( $< 15$ ) for basaltic rocks support minimal crustal contamination (Hart et al. 1989; Saunders et al., 1992). In addition, the samples plot along higher Th/Yb and Ta/Yb values, indicating the presence of garnet-bearing residue in the mantle source and (or) low degree partial melting.

To test the contribution of the subduction component, N-MORB-normalized HFSE / LREE, especially Nb/Ce, variation diagrams have been produced and  $(\text{Nb}/\text{Ce})_N$  ratios are shown in Fig. 9B. The diagram of  $\text{Ce}_N$  against  $\text{Nb}_N$  (where the subscript N denotes normalization to N-type MORB) best highlights the differing source enrichment processes. While positive Nb anomalies relative to Ce (relatively high  $(\text{Nb}/\text{Ce})_N$  ratios) indicate within plate processes

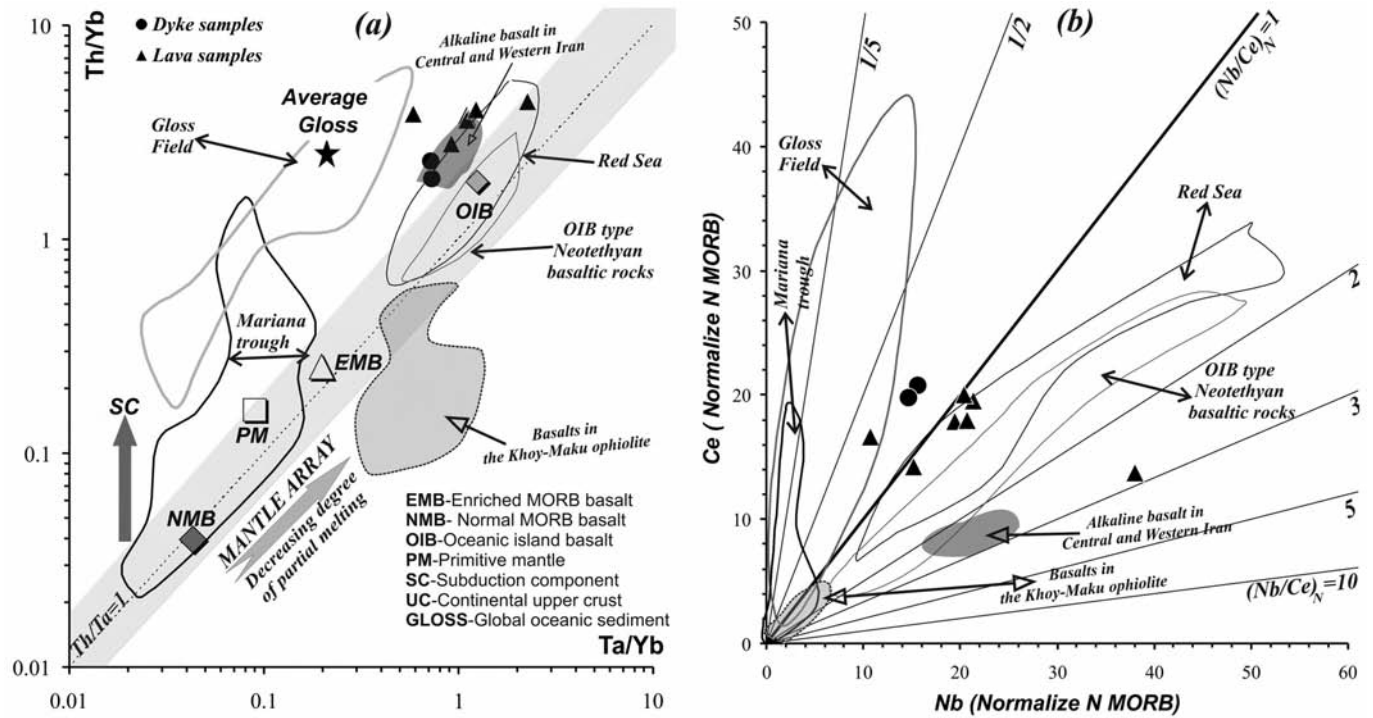


Fig. 9 - Trace element diagrams for petrogenesis of the studied samples. (a) Ta/Yb against Th/Yb diagram (b) Nb/Ce (after Pearce 1983). Oceanic island basalt (OIB), mid ocean ridge basalt (NMB), enrichment MORB (EMB), Primitive Mantle (PM) compositions are from Sun and McDonough (1989). Global oceanic sediment (GLOSS; Plank and Langmuir 1998), Mariana trough (Pearce et al., 2005; Peate and Pearce 1998), Red Sea (Volker et al., 1997; Rogers 1993), and NW Anatolian Neotethyan basaltic rocks (Aldanmaz et al., 2006) have been plotted for comparison on both diagrams. For the geochemical data from Iran see text.

(OIB;  $(Nb/Ce)_N = 1.931$ , Sun and McDonough, 1989), mantle sources enriched by a subduction component are characterized by negative Nb anomalies with respect to Ce (Mariana arc lavas;  $(Nb/Ce)_N = 0.3-0.7$  Pearce et al., 2005). Nb/Ce ratios of all samples range from 0.5 to 3. This implies that the mantle source region of the studied samples could be derived from a mixture of a mantle source slightly enriched by a subduction component and an OIB-like mantle source.

Shervais (1982) reported that alkaline rocks (or OIB like lavas) generally have Ti/V ratios  $> 50$ . High Ti/V (40-105) and low Y/Nb (0-1) ratios of the studied samples indicate that they were derived from a source similar to OIB-like mantle. Therefore, in the Ti/1000 vs V diagram of Shervais (1982), dyke and lava samples with high Ti/V ratios implies that they were formed from a within plate or from an OIB-like mantle source (Fig. 10).

As discussed above, LILE, LREE and HFSE contents as well as multi-element patterns of the dykes and lava samples reflect a mantle source slightly enriched with a subduction component. HFSE and HREE concentrations of the samples can be used to identify the mantle source region prior to enrichment and (or) metasomatism. Nb, Ta, Zr, Hf, Yb and Y elements are immobile in fluids and are unaffected by subduction-related enrichment processes (Pearce and Parkinson, 1993; Pearce et al., 2005). For this reason, Nb/Ta vs. Zr/Nb variation diagrams were created with fields of typical OIB, MORB and SSZ (supra-subduction zone) type volcanic rocks for comparison. These diagrams support the interpretation obtained from the Shervais (1982) diagrams indicating an OIB-like mantle source (Fig. 11A). In addition, Y/Ce versus Nb/Zr diagrams (Fig. 11B) suggests that they can be formed by low degree partial melting and from an OIB-like mantle source.

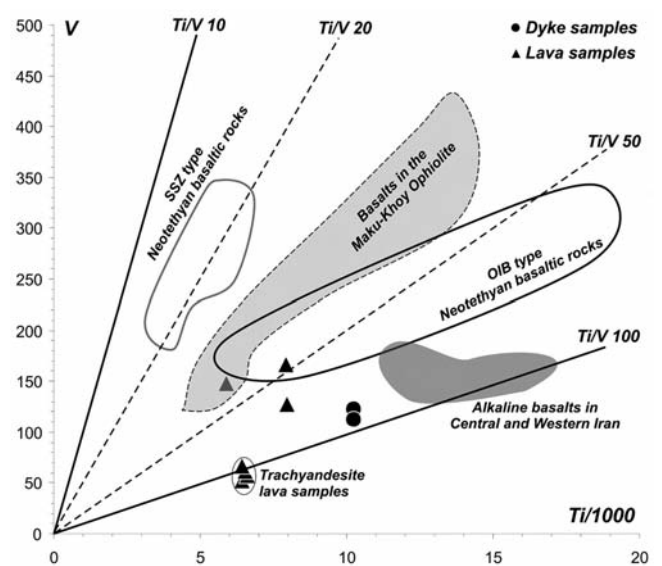


Fig. 10 - Ti versus V diagram (after Shervais 1982). Data source for SSZ-type and OIB type Neotethyan basaltic rocks are from Aldanmaz et al. (2006), the shaded areas represents the coeval subalkaline and alkaline basalts of W Iran (for geochemical data see text).

### Partial melting

In order to evaluate the nature of the mantle sources and partial melting processes of the studied samples, we carried out a partial melting modelling using REE geochemistry. REE ratios of the lavas are useful to reflect the extent, depth and degree of partial melting based on the mineralogy and

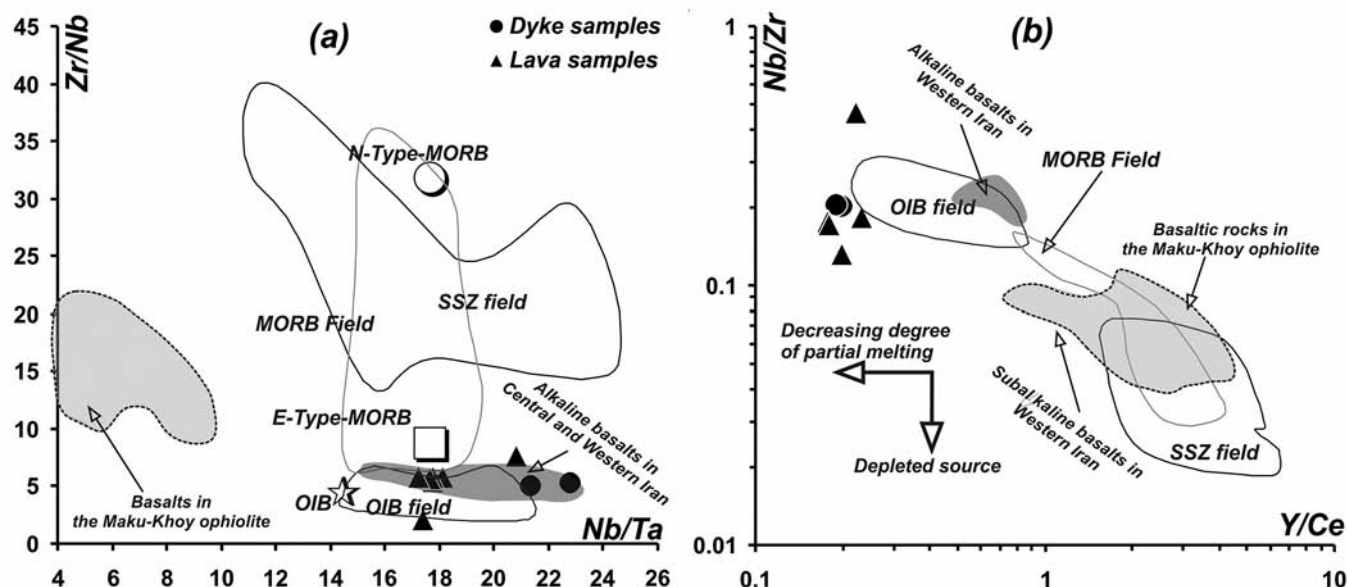


Fig. 11 - Trace element variation diagrams for mantle source region of studied rocks. (a) Nb/Ta vs Zr/Nb, (b) Y/Ce vs Nb/Zr diagrams. OIB, N-MORB, Enriched MORB (E-MORB) compositions are from Sun and McDonough (1989). OIB, MORB and SSZ fields are from Aldanmaz et al. (2006). Shaded areas are from W Iran (for geochemical data see text).

chemistry of the source facies since solid-melt partitioning these elements are different for garnet- and spinel-lherzolites (Thirlwall et al., 1994; Shaw et al., 2003). Enrichment of MREE, (e.g., Tb, Dy) with respect to HREE (e.g., Yb) occurs if garnet is the residual phase during partial melting, as HREE are dominantly retained by garnet (High  $D_{Yb} \sim 4-44$ ; Shaw et al., 2003).

Hence, low degrees of partial melting within the garnet facies produces high MREE / HREE ratios and differences between melt and source ratios (Garnet - melt  $D_{Yb} \sim 4$ ; Garnet - melt  $D_{MREE} \sim 0.21-1$  McKenzie and O'Nions, 1991). In contrast, melting in the spinel facies will generate little change in MREE / HREE ratios with similar melt and source ratios (Spinel - melt  $D_{Yb} \sim 0.01$ ; Spinel - melt  $D_{MREE} \sim 0.01$ ; McKenzie and O'Nions, 1991).

Fig. 12 shows a  $(Yb)_N$  versus  $(Dy/Yb)_N$  diagram for the studied samples along with modeled trajectories for non-modal batch melting of spinel, garnet and garnet-spinel peridotite sources. We use two source concentrations for modeling: i) depleted MORB mantle (DMM; Workman and Hart, 2005) that is representative of convecting asthenospheric mantle source and, ii) primitive mantle (PM; Sun and McDonough, 1989) source representing the initial mantle composition.

Neither the PM nor the DMM compositions can generate the observed features of the studied samples along the melting curves for the spinel and garnet peridotite facies (Fig. 12). To make an assumption for producing the mantle source of our samples we mix PM and DMM sources using equations from Langmuir et al. (1978). The best-fit curve generated by applying non-modal batch melting to a garnet-spinel bearing mantle source mixture of 70% PM and 30% DMM sources in Fig. 12, reproduces the characteristics of the studied samples. Our model indicates that the samples are the result of 1-4% melting of a mixed mantle source.

The overall petrogenetic evaluation suggests that, during the subduction of the oceanic lithosphere, the subduction-modified mantle of the hanging wall may have been affected

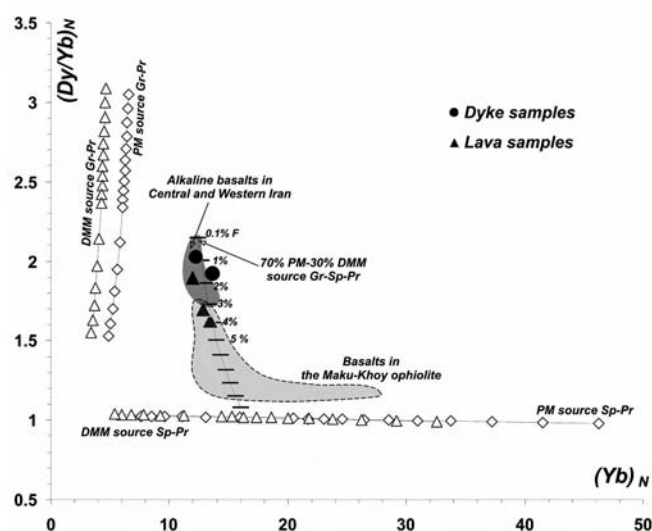


Fig. 12 -  $(Yb)_N$  vs  $(Dy/Yb)_N$  for studied samples and non modal batch melting modeling of peridotitic mantle sources. In order to minimize the effect of contamination and crystallization, only most primitive samples are plotted. Melt curves are obtained using non modal batch melting equations of Shaw (1970). Values are chondrite-normalized after Sun and McDonough (1989). The thick marks on the curves indicate the degree ( $F$ ) of partial melting. Partition coefficients are from McKenzie and O'Nions (1991). PM and DMM compositions are from Sun and McDonough (1989) and Workman and Hart (2005), respectively. The shaded areas represent the alkaline and subalkaline fields of W Iran for geochemical data see text). Garnet peridotite (Gr-Pr) composition: 0.6 ol, 0.2 opx, 0.1 cpx, 0.1 gr, that melts in the proportions 0.03 ol, 0.16 opx, 0.88 cpx, 0.09 gr (Walter, 1998); spinel peridotite (Sp-Pr): 0.53 ol, 0.27 opx, 0.17 cpx, 0.03 sp, that melts in the proportions 0.06 ol, 0.28 opx, 0.67 cpx, 0.11 sp (Kinzler, 1997). Garnet-spinel peridotite has a modal mineralogy of 0.55 ol, 0.24 opx, 0.15 cpx, 0.04 gr, 0.02 sp, that melts in the proportions of 0.05 ol, 0.05 opx, 0.28 cpx, 0.35 gr, 0.27 sp.

by a small degree of partial melting due to slab retreat (Fig. 13). The upwelling of OIB-like asthenospheric material during retreat of the subducting slab would have resulted in generation of a mixed source for the volcanics in the region consisting of a of subduction modified source and the enriched asthenospheric melts in the back-arc region, as shown by the non modal batch melting model in Fig. 12. Only a limited amount of melting (1-4%) is needed to produce the lavas and the dykes found in the study area.

A comparison of the volcanic rocks of the study area with the coeval subalkaline and alkaline basalts of southern Iran (Ghazi and Hassanipak, 1999) shows that the alkaline volcanics are very similar in their petrological characteristics to the lavas of the study area (see Figs. 6, 7, 9, 10 and 11 and the following chapters) and were very probably formed by similar processes during the Late Cretaceous.

### GEOLOGICAL IMPLICATIONS FOR THE EVOLUTION OF BERIT-ELAZIĞ-VAN OPHIOLITIC BELT OF SOUTHERN NEOTETHYS

Ophiolitic bodies with preserved pseudo-stratigraphy (e.g., the Guleman ophiolite) were known as distinct tectonic units along the southern Neotethyan suture since the pioneering studies of the 1950's (e.g., Kaaden, van der, 1959). Subsequent studies examining the geochemistry of the mantle rocks as well as volcanic rocks of oceanic crust origin resulted in the recognition of "ensimatic arc" assemblages (e.g., Michard et al., 1984). More recent work, based upon detailed petrological data coupled with radiometric age dating, was mainly concentrated on the Malatya-Elazığ regions and provided evidence for "supra-subduction-type" oceanic crust generation along the northern branch of Southern Neotethys during the Middle to Late Mesozoic (e.g., Ural et al., 2010; Karaoğlan, et al., 2013; 2014 and references therein). These rocks were included in the "Yüksekova Arc Complex" by Perinçek (1990). However, the scarcity of age data coupled with the tectono-magmatic characteristics of the volcanism prevented a detailed evaluation of the oceanic crustal evolution. Moreover, to the east of Malatya-Elazığ area, the tectono-magmatic features and age of the ophiolitic

bodies close to the Iranian border were not known until the recent work of Çolakoğlu et al. (2012). The data obtained by Çolakoğlu et al. (2012), together with the data presented here, has a number of important regional geological implications regarding the closure of the southern Neotethys.

First of all, the new data confirms the previous interpretations that the demise of the Berit-Elazığ-Van ophiolitic belt includes remnants of an oceanic branch that was formed by intra-oceanic subduction. This is validated by geochemical data from the oceanic basalts combined with ages obtained from associated sediments. The oldest ages yet obtained from island-arc-type lava-radiolarian chert association was Santonian (Ural et al., 2010), indicating that the intra-oceanic subduction has started earlier than ca. 85 Ma. This finding is also confirmed by the Ar/Ar age of 87 Ma from SSZ-type dykes, which cross-cut the mantle rocks just to the west of the studied area in this paper (Alabayir ophiolite; Çolakoğlu et al., 2012).

To the east, across the Turkish-Iranian border, oceanic assemblages associated with Late Cretaceous sediments occur in the Khoy ophiolitic complex (Ghazi et al., 2003; Khalatbari-Jafari et al., 2004; 2006; Pessagno et al., 2005). The "pelagic fossiliferous carbonates and basalts as interlayers or exotic blocks" yielded Late Cretaceous (late Campanian) to Middle to Late Eocene planktonic foraminifera (Ghazi et al., 2003). The petrological data of Hassanipak and Ghazi (2000) from the Khoy complex suggests the presence of massive and pillow basalts with E-MORB and transitional E-MORB - N-MORB characteristics, respectively. The dominating MORB character is also confirmed by Khalatbari-Jafari et al. (2006), who excluded a possible supra-subduction setting. By this, the geochemical character of the Khoy basalts differs from the SSZ basalts of the Elazığ-Van suture zone as clearly seen on Figs. 7, 9, 10 and 11.

Another ophiolitic body with a much better comparable geochemistry is the Kermanshah ophiolitic complex. Together with other ophiolitic bodies (e.g., Naien, Baft, Esphandagheh and Shahr Babak ophiolites) they are located along the Inner Zagros Belt of Southern Neotethys. The Sanandaj-Sirjan Belt is the equivalent of the Bitlis-Pütürge metamorphic zone in Turkey. As it is the case in Bitlis-Pütürge (Hall, 1980; Göncüoğlu and Turhan, 1983; 1984)

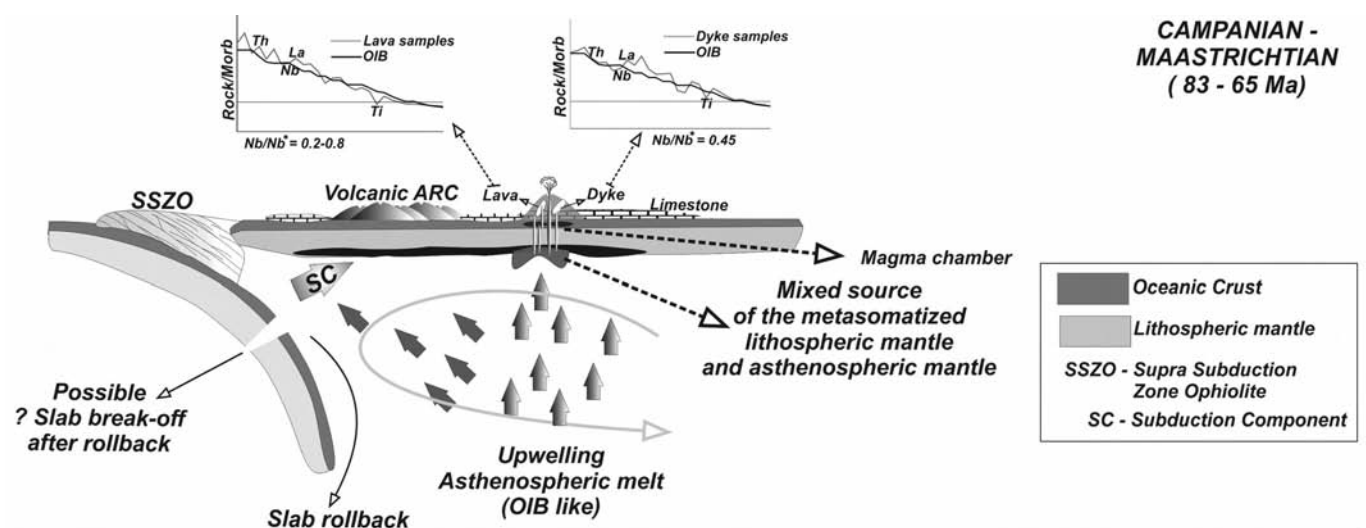


Fig. 13 - Model for the formation of late Maastrichtian volcanics within the intra-oceanic subduction zone in the eastern Elazığ-Van segment of the Southern Neotethys.

the Kermanshah ophiolite is sandwiched between the metamorphic units of the Sanandaj-Sirjan and the Zagros belts (Ghasemi and Talbot, 2006; Moghadam et al., 2010; Moghadam and Stern, 2011).

In Kermanshah ophiolite, Ghazi and Hassanipak (1999) identified both subalkaline and alkaline basalts, which were derived from basaltic melts generated in island arc and intra-oceanic plate environments, respectively. In the Kermanshah and NE Irak ophiolites, alkaline (or, more generally, enriched) rocks are also described by Saccani et al. (2013) and Saccani et al. (2014), respectively. They do not show any Ti and Nb negative anomalies and are interpreted as forming at the ocean-continent transition zone during the early drift phase of the Southern Neo-Tethys (e.g., Robertson, 2007) during the Late Triassic-?Early Jurassic. This interpretation further emphasises the important difference in Ti, Nb concentration between the Late Cretaceous Van ophiolites and the Triassic Iranian rocks and support our hypothesis of formation of the Van ophiolites in a back arc basin during Late Cretaceous. The distinct IAT component in several types of basalts of the Shahr-Babak ophiolites by several authors (e.g., Campbell et al., 1999 and Ghazi and Hassanipak, 1999) and Moghadam et al. (2013) suggestion, that most Gogher-Baft ophiolite magmatic rocks show supra-subduction zone affinities is another clue for the continuation of Elazığ-Van ophiolites towards east.

A geochemical correlation of alkaline and subalkaline basalts of the southern Iranian ophiolitic basalts with those of the eastern Berit-Elazığ-Van ophiolitic belt is shown in Figs. 6, 8, 9, and 10. From these it is obvious that the alkaline basalts are petrologically similar and may have been formed by similar processes in a similar tectonic setting.

Combining the data from our studies on oceanic basalts between Elazığ and the Iranian border (Çolakoğlu et al., 2012; Ural et al., 2013, and this study) are formed in general by various settings such as fore-arc, arc and back arc above a subducting Neotethyan oceanic lithosphere.

## CONCLUSIONS

The preliminary geochemical and paleontological age data obtained from a lava-radiolarian chert association in the Berit-Elazığ-Van ophiolitic belt helps to reconstruct the closure of the Elazığ-Van segment of the southern Neotethys. These new findings suggest that the southern Neotethyan oceanic basin between the Bitlis Pütürge/Sanandaj-Sirjan belt and the Tauride-Anatolide/Central Iranian belt closed by intra-oceanic subduction. The oldest ages obtained from the arc/back-arc basalts in the Elazığ area suggest that intra-oceanic decoupling was already in progress during the Santonian (e.g., Ural et al., 2010). This finding is confirmed by the Ar/Ar ages of the isolated diabase dykes (105-92 Ma) from Van area. The new finding of late Maastrichtian SSZ-type volcanism at the Turkish-Iranian border (this study) as well as further east (e.g., Moghadam et al., 2013) suggests that the Elazığ-Van-Inner Zagros belt was the main locus of the subduction-accretion during the end of Cretaceous.

A further implication of the recent finding is that the recently identified oceanic basalts represent the youngest SSZ-type volcanism yet proven in SE Anatolia. Younger ages were only encountered in the sediments of Paleocene and Eocene olistostromes (Seske Formation) that reworked the Yüksekova mélangé (e.g., Şenel et al., 1984). By the absence of younger oceanic crust generation, there is no reli-

able data for the previously suggested models (e.g., Şengör and Yılmaz, 1981) advocating an open ocean during the Early Tertiary.

## ACKNOWLEDGMENTS

The authors are thankful to Prof. U.K. Tekin and U. Çakır for their contributions during the fieldwork. This study was granted by Yüzüncü Yıl University/ Project number is BAP 2010-FBE-D052. The authors acknowledge Dr. K. Sayit and Dr. H.S. Moghadam for their comments on the former version of this paper. Dr. E Saccani and Dr. L. Pandolfi are acknowledged for their review.

## REFERENCES

- Acarlar M., Bilgin A., Erkal T., Güner E., Şen A., Umut M., Elibol E., Gedik İ., Hakyemez Y. and Uğuz F., 1991. Van Gölü ve Kuzeyinin jeolojisi. M.T.A Report, Nr. 9469 (unpublished). Van.
- Adam J. and Green T., 2006. Trace element partitioning between mica- and amphibole-bearing garnet lherzolite and hydrous basanitic melt: 1. Experimental results and the investigation of controls on partitioning behavior. *Contrib. Mineral. Petrol.*, 152: 1-17.
- Aldanmaz E., Yalınız M.K., Güçtekin A. and Göncüoğlu M.C., 2006. Geochemical characteristics of mafic lavas from the Neotethyan ophiolites in western Turkey: implications for heterogeneous source contribution during variable stages of ocean crust generation. *Geol. Mag.*, 145: 37-54.
- Bağcı U., Parlak O. and Höck V., 2005. Whole rock and mineral chemistry of cumulates from the Kızıldağ (Hatay) ophiolite (Turkey): clues for multiple magma generation during crustal accretion in the southern Neotethyan ocean. *Min. Mag.*, 69: 53-76.
- Bienvenu P., Bougault H., Joron J.L., Treuil M. and Demitriev L., 1990. MORB alteration: rare-earth element/non rare-earth hygromagmaphile element fractionation. *Chem. Geol.*, 82: 1-14.
- Blome C.D. and Irwin W.P., 1985. Equivalent radiolarian ages from ophiolitic terranes of Cyprus and Oman. *Geology*, 13: 401-404.
- Brenan J.M., Shaw H.F., Ryerson F.J. and Phinney D.L., 1995. Mineral-aqueous fluid partitioning of trace elements at 900°C and 2.0 GPa: constraints on the trace element chemistry of mantle and deep crustal fluids. *Geochim. Cosmochim. Acta*, 59: 3331-3350.
- Campbell K., Ghazi A.M., LaTour T. and Hassanipak A.A., 1999. Geochemistry, petrology and tectonics of the Shahr-Babak ophiolite, SE Iran. *Geol. Soc. Am., SE Sect. Abstr. Progr.*, 31 (9): 485-497.
- Çolakoğlu A.R., Sayit K., Günay K. and Göncüoğlu M.C., 2012. Geochemistry of mafic dykes from the Southeast Anatolian ophiolites, Turkey: Implications for an intra-oceanic arc-basin system. *Lithos*, 132-133: 113-126.
- Dilek Y. and Thy P., 2009. Island arc tholeiite to boninitic melt evolution of the Cretaceous Kizildag (Turkey) ophiolite: Model for multi-stage early arc-forearc magmatism in Tethyan subduction factories. *Lithos*, 113: 68-87.
- Dilek Y., Imamverdiyev N. and Altunkaynak S., 2010. Geochemistry and tectonics of Cenozoic volcanism in the Lesser Caucasus (Azerbaijan) and the peri-Arabian region: collision-induced mantle dynamics and its magmatic fingerprint. *Int. Geol. Rev.*, 52: 536-578.
- Elmas A., 1992. Geological investigation of Erçek Lake (Van) area. Unpubl. Ph.D. thesis, Univ. Istanbul, 372 pp.
- Elmas A. and Yılmaz Y., 2003. Development of an oblique subduction zone/Tectonic evolution of the Tethys suture zone in Southeast Turkey. *Int. Geol. Rev.*, 45: 827-840.
- Floyd P.A. and Winchester J.A., 1978. Identification and discrimination of altered and metamorphosed volcanic rocks using immobile elements. *Chem. Geol.*, 21: 291-306.

- Ghasemi A. and Talbot C.J., 2006. A new tectonic scenario for the Sanandaj-Sirjan Zone (Iran). *J. Asian Earth Sci.*, 26: 683-693.
- Ghazi A.M. and Hassanipak A.A., 1999. Geochemistry of subalkaline and alkaline extrusives from the Kermanshah ophiolite, Zagros Suture Zone, Western Iran: implications for Tethyan plate tectonics. *J. Asian Earth Sci.*, 17: 319-332.
- Ghazi A.M., Pessagno E.A., Hassanipak A.A., Kariminia S.M., Duncan R.A. and Babaie H.A., 2003. Biostratigraphic zonation and  $^{40}\text{Ar}$ - $^{39}\text{Ar}$  ages for the Neotethyan Khoy ophiolite of NW Iran. *Palaeo. Palaeo. Palaeo.*, 193: 311-323.
- Göncüoğlu M.C., 2010. Introduction to the geology of Turkey: Geodynamic evolution of the pre-Alpine and Alpine terranes. General Directorate of Mineral. Res. Explor., Monography Series, 5: 1-66 (ISBN 978-605-4075-74)
- Göncüoğlu M.C. and Turhan N., 1983. New results on the age of Bitlis Metamorphics. *MTA Dergisi*, 95-96:1-5.
- Göncüoğlu M.C. and Turhan N., 1984. Geology of the Bitlis Metamorphic Belt. In: O. Tekeli and M.C. Göncüoğlu (Eds.), *Int. Symp. Geology of the Taurus Belt, Proceed.*, p. 237-244
- Göncüoğlu M.C., Dirik K. and Kozlu H., 1997. General characteristics of pre-Alpine and Alpine terranes in Turkey: Explanatory notes to the terrane map of Turkey. *Ann. Géol. Pays Hellén.*, 37: 515-536.
- Hall R., 1980. Unmixing a mélange: the petrology and history of a disrupted and metamorphosed ophiolite, SE Turkey. *J. Geol. Soc. London*, 137: 195-206.
- Hart W.K., Wolde G., Walter R.C. and Mertzman S.A., 1989. Basaltic volcanism in Ethiopia: constraints on continental rifting and mantle interactions. *J. Geophys. Res.*, 94: 7731-7748.
- Hassanipak A.A. and Ghazi A.M., 2000. Petrology, geochemistry and tectonic setting of the Khoy ophiolite, northwest Iran: implications for Tethyan tectonics. *J. Asian Earth Sci.*, 18 (1): 109-121.
- Hawkesworth C.J., Gallagher K., Hergt J.M. and McDermott F., 1993. Mantle and slab contributions in arc magmas. *Ann. Rev. Earth Planet. Sci.*, 21: 175-204.
- Hawkesworth C.J., Turner S.P., McDermott F., Peate D.W. and Van Calsteren P., 1997. U-Th isotopes in arc magmas: implications for element transfer from the subducted crust. *Science*, 276: 551-555.
- Hofmann A.W., 1986. Nb in Hawaiian magmas: constraints on source composition and evolution. *Chem. Geol.*, 57: 17-30.
- Hofmann A.W., 1988. Chemical differentiation of the Earth: the relationship between mantle, continental crust, and the oceanic crust. *Earth Planet. Sci. Lett.*, 90: 297-314.
- Hofmann A.W., 1997. Mantle geochemistry: the message from oceanic volcanism. *Nature*, 385: 219-229.
- Irving A.J. and Frey F.A., 1978. Distribution of trace-elements between garnet megacrysts and host volcanic liquids of kimberlitic to rhyolitic composition. *Geochim Cosmochim. Acta*, 42: 771-787.
- Kaaden G., Van der, 1959. On relationship between the composition of chromites and their tectonic-magmatic position in the peridotite bodies in the SW of Turkey. *Bull. Mineral Res. Explor.*, 52: 1-15.
- Karaoğlu F., Parlak O., Klötzli U., Köller F. and Rızaoğlu T., 2013. Age and duration of intra-oceanic arc volcanism built on a suprasubduction zone type oceanic crust in Southern Neotethys, SE Anatolia. *Geosci. Frontiers*, 4: 399-408.
- Karaoğlu F., Parlak O., Klötzli U., Thöni M. and Köller F., 2014. U-Pb and Sm-Nd geochronology of the ophiolites from the SE Turkey: implications for the Neotethyan evolution. *Geodin. Acta*, 25: 146-161.
- Keppeler H., 1996. Constraints from partitioning experiments on the composition of subduction zone fluids. *Nature*, 380: 237-240.
- Keskin M., Pearce J.A. and Mitchell J.G., 1998. Volcano-stratigraphy and geochemistry of collision-related volcanism on the Erzurum-Kars Plateau, North Eastern Turkey. *J. Volcan. Geotherm. Res.*, 8: 355-404.
- Ketin İ., 1977. Van Gölü ile İran sınırı arasındaki bölgede yapılan jeolojik gözlemlerinin sonuçları hakkında kısa bir açıklama. *Bull. Geol. Soc. Turkey*, 20: 79-85.
- Khalatbari-Jafari M., Juteau T., Bellon H., Whitechurch H., Cotten J. and Emami H., 2004. New geological, geochronological and geochemical investigations on the Khoy ophiolites and related formations, NW Iran. *J. Asian Earth Sci.*, 23:507-535.
- Khalatbari-Jafari M., Juteau T. and Cotten J., 2006. Petrological and geochemical study of the Late Cretaceous ophiolite of Khoy (NW Iran), and related geological formations. *J. Asian Earth Sci.*, 27: 465-502.
- Kinzler R.J., 1997. Melting of mantle peridotite at pressures approaching the spinel to garnet transition: application to mid ocean ridge basalt petrogenesis. *J. Geophys. Res.*, 102: 853-874.
- Langmuir C.H., Vocke Jr. R.D. and Hanson G.N., 1978. A general mixing equation with applications to Icelandic basalts. *Earth Planet. Sci. Lett.*, 37: 380-392.
- MacLean W.H. and Barret T.J., 1993. Litho-geochemical techniques using immobile elements. *J. Geochem. Explor.*, 48: 109-133.
- Mc Kenzie D.P. and O'Nions R.K., 1991. Partial melt distributions from inversion of rare earth element concentrations. *J. Petrol.*, 32: 1021-1091.
- Meschede M., 1986. A method of discriminating between different types of mid-ocean ridge basalts and continental tholeiites with the Nb-Zr-Y diagram. *Chem. Geol.*, 56: 207-263.
- Michard A., Whitechurch H., Ricou L.E., Montigny R. and Yazgan E., 1984. Tauric subduction (Malatya-Elazığ provinces) and its bearing on tectonics of the Tethyan realm in Turkey. In: A.H.F. Robertson and A.J.F. Dixon (Eds.), *Geol. Soc. London Spec. Publ.*, 17: 361-373.
- Moghadam H.S. and Stern R.J., 2011. Geodynamic evolution of Upper Cretaceous Zagros ophiolites: formation of oceanic lithosphere above a nascent subduction zone. *Geol. Mag.*, 148: 762-801.
- Moghadam H.S., Stern R.J., Chiaradia M. and Rahgoshay M., 2013. Geochemistry and tectonic evolution of the Late Cretaceous Gogher-Baft ophiolite, central Iran. *Lithos*, 168: 33-47.
- Moghadam H.S., Stern R.J. and Rahgoshay M., 2010. The Dehshir ophiolite (central Iran): Geochemical constraints on the origin and evolution of the Inner Zagros ophiolite belt. *Geol. Soc. Am. Bull.*, 122: 1516-1547.
- Oberhaensli R., Candan O., Çetinkaplan M., Koralay E. and Bousquet R., 2012. The East Anatolian high-temperature belt. *Proceed. 65<sup>th</sup> Geol. Congress, Abstr. Vol.*, p. 87.
- Parlak O., Karaoğlu F., Thoni M., Robertson A.H.F., Okay A.I. and Köller F., 2012. Geochemistry, geochronology and tectonic significance of HT meta-ophiolitic rocks. possible relation to Eocene South-Neotethyan arc magmatism (Malatya Area, SE Anatolia). *Proceed. 65<sup>th</sup> Geol. Congress*, p. 90-91.
- Parlak O., Rızaoğlu T., Bağcı U., Karaoğlu F. and Höck V., 2009. Tectonic significance of the geochemistry and petrology of ophiolites in southeast Anatolia, Turkey. *Tectonophysics*, 473: 173-187.
- Pearce J.A., 1983. The role of sub-continental lithosphere in magma genesis at destructive plate margins. In: C.J. Hawkesworth and M.J. Norry (Eds.), *Continental basalts and mantle xenoliths*, Cheshire, United Kingdom, Shiva Publishing, p. 230-249.
- Pearce J.A. and Cann J.R., 1973. Tectonic setting of basic volcanic rocks determined using trace element analyses. *Earth Planet. Sci. Lett.*, 19: 290-300.
- Pearce J.A. and Norry M.J., 1979. Petrogenetic implications of Ti, Zr, Y and Nb variations in volcanic rocks. *Contrib. Mineral. Petrol.*, 69: 33-47.
- Pearce J.A. and Parkinson I.J., 1993. Trace element models for mantle melting: application to volcanic arc petrogenesis. In: H.M. Prichard, T. Alabaster, N.B.W. Harris and C.R. Neary (Eds.), *Magmatic processes and plate tectonics*. *Geol. Soc. London Spec. Publ.*, 76: 373-403.
- Pearce J.A. and Peate D.W., 1994. Tectonic implications of the composition of volcanic arc magmas. *Ann. Rev. Earth Planet. Sci.*, 123: 251-285.
- Pearce J.A., Stern R.J., Bloomer H.S. and Fryer P., 2005. Geochemical mapping of the Mariana arc-basin system: Implications for the nature and distribution of subduction components. *Geochem. Geophys. Geosyst.*, 6: 1-27.
- Peate D.W. and Pearce J.A., 1998. Causes of spatial compositional variations in Mariana arc lavas: Trace element evidence. *Island Arc*, 7: 479-495.

- Perinçek D., 1990. Stratigraphy of the Hakkari province, Southeast Turkey. *Bull. Turk. Ass. Petrol. Geol.*, 2: 21-68.
- Pessagno E.A., Ghazi A.M., Kariminia M., Duncan R.A. and Hassanipak A.A., 2005. Tectonostratigraphy of the Khoys Complex, northwestern Iran. *Stratigraphy*, 2: 49-63.
- Plank T. and Langmuir C.H., 1998. The chemical composition of subducting sediment and its consequences for the crust and mantle. *Chem. Geol.*, 145: 325-394.
- Robertson A.H.F., 2002. Overview of the genesis and emplacement of Mesozoic ophiolites in the Eastern Mediterranean Tethyan region. *Lithos*, 65: 1-67.
- Robertson A.H.F., 2006. Contrasting modes of ophiolite emplacement in the Eastern Mediterranean region: In: D. Gee and R.A. Stephenson (Eds.), *European lithosphere dynamics*. *Geol. Soc. London Mem.*, 32: 233-256.
- Robertson A.H.F., 2007. Overview of tectonic settings related to the rifting and opening of Mesozoic ocean basins in the Eastern Tethys: Oman, Himalayas and Eastern Mediterranean regions. In: G. Karner, G. Manatschal and L. Pinheiro (Eds.), *Imaging, mapping and modelling continental lithosphere extension and breakup*. *Geol. Soc. London Spec. Publ.*, 282: 325-389.
- Robertson A.H.F., Parlak O. and Ustaömer T., 2012. Overview of the Palaeozoic-Neogene evolution of Neotethys in the Eastern Mediterranean region (southern Turkey, Cyprus, Syria). *Petrol. Geosci.*, 18: 381-404.
- Robertson A.H.F., Parlak O. and Ustaömer T., 2013. Late Palaeozoic-Early Cenozoic tectonic development of Southern Turkey and the easternmost Mediterranean region: Evidence from the inter-relationships of continental and oceanic units. In: A.H.F. Robertson O., Parlak and U.C. Ünlügenç (Eds.), *Geological development of the Anatolian continent and the easternmost Mediterranean basin*. *Geol. Soc. London Spec. Publ.*, 372: 9-48.
- Rogers N.W., 1993. The isotope and trace element geochemistry of basalts from the volcanic islands of the southern Red Sea. In: H.M. Prichard, T. Alabaster, N.B.W. Harris and C.R. Neary (Eds.), *Magmatic processes and plate tectonics*. *Geol. Soc. London Spec. Publ.*, 76: 455-467.
- Rolland Y., Perinçek D., Kaymak N., Sosson M., Barrier E. and Avagyan A., 2011. Evidence for 80-75 Ma subduction jump during Anatolide-Tauride-Armenian block accretion and 48 Ma Arabia-Eurasia collision in Lesser Caucasus-East Anatolia. *J. Geodyn.*, 56-57: 76-85.
- Saccani E., Allahyari K., Beccaluva L. and Bianchini G., 2013. Geochemistry and petrology of the Kermanshah ophiolites (Iran): Implication for the interaction between passive rifting, oceanic accretion, and plume-components in the Southern Neotethys Ocean. *Gondwana Res.*, 24: 392-411.
- Saccani E., Allahyari K. and Rahimzadeh B., 2014. Petrology and geochemistry of mafic magmatic rocks from the Sarve-Abad ophiolites (Kurdistan region, Iran): Evidence for interaction between MORB-type asthenosphere and OIB-type components in the southern Neo-Tethys Ocean. *Tectonophysics*, 621: 132-147.
- Saunders A.D., Storey M., Kent R.W. and Norry M.J., 1992. Consequences of plume-lithosphere interactions: In: B.C. Storey, T. Alabaster and R.J. Pankhurst (Eds.), *Magmatism and the causes of continental break-up*. *Geol. Soc. London Spec. Publ.*, 68: 41-60.
- Şenel M., Acarlar M., Çakmakçoğlu A., Erkanol D., Taşkıran M.A., Ulu Ü., Ünal M.F., Örcen S., Yıldırım H. and Dağ Z., 1984. Geology of the area between Özalp (Van) and the Iranian border. M.T.A Genel Müdürl. Jeol. Dairesi, (Unpubl.) Report, Nr 663, Ankara.
- Şenel M. and Ercan T., 2002. Geological map of Turkey, 1/500.000, the Van Sheet. General Directorate of Mineral Res. Explor., Ankara, 2<sup>nd</sup> ed.
- Şengör A.M.C., 1984. The Cimmeride orogenic system and the tectonics of Eurasia. *Geol. Soc. Am. Spec. Pap.*, 195: 1-74.
- Şengör A.M.C. and Yılmaz Y., 1981. Tethyan evolution of Turkey: a plate tectonic approach. *Tectonophysics*, 75: 181-241.
- Şengör A.M.C., Özeren S., Genç T. and Zor E., 2003. East Anatolian high plateau as a mantle-supported, north-south shortened domal structure. *Geophys. Res. Lett.*, 30 (24): 8045.
- Şengör A.M.C., Özeren M.S., Keskin M., Sakiç M., Özbakır A.D. and Kayan İ., 2008. Eastern Turkish high plateau as a small Turkic-type orogen: Implications for post-collisional crust-forming processes in Turkic-type orogens. *Earth Sci. Rev.*, 90: 1-48.
- Şengör A.M.C., White G.W. and Dewey J.F., 1979. Tectonic evolution of the Bitlis Suture, southeastern Turkey: implications for the tectonics of the eastern Mediterranean. *Rapp. Comm. Int. Mer Medit.*, 25/26 (2a): 95-97.
- Shaw D.M., 1970. Trace element fractionation during anatexis. *Geochim. Cosmochim. Acta*, 34: 237-243.
- Shaw J.E., Baker J.A., Menzies M.A., Thirlwall M.F. and İbrahim K.M., 2003. Petrogenesis of the largest intraplate volcanic field on the Arabian Plate (Jordan): a mixed lithosphere-asthenosphere source activated by lithospheric extension. *J. Petrol.*, 44: 1657-1679.
- Shervais M., 1982. Ti-V plots and the petrogenesis of modern and ophiolitic lavas. *Earth Planet. Sci. Lett.*, 59: 101-118.
- Sun S.S. and McDonough W.F., 1989. Chemical and isotopic systematics of oceanic basalts: implications for mantle composition and processes. In: A.D. Saunders and M.J. Norry (Eds.), *Magmatism in the ocean basins*. *Geol. Soc. London Spec. Publ.*, 42: 45-313.
- Thirlwall M.F., Upton B.G.J. and Jenkins C., 1994. Interaction between continental lithosphere and the Iceland plume - Sr-Nd-Pb isotope geochemistry of Tertiary basalts, NE Greenland. *J. Petrol.*, 35: 839-879.
- Turner S., Bourdon B. and Gill J., 2003. Insight into magma genesis at convergent margins from U-series isotopes: In: B. Bourdon, G.M. Henderson, C.C. Lundstrom and S.P. Turner (Eds.), *Uranium-series geochemistry. Reviews in Mineralogy and Geochemistry*. *Mineral. Soc. Am.*, 52: 255-310.
- Ural M., Kürüm S., Arslan M., Gönçüoğlu M.C. and Tekin U.K., 2010. Petrographical and petrochemical features of Upper Cretaceous pillow lavas from Elazığ and Malatya areas, SE Turkey. *Geophys. Res. Abstr.*, 2: 11662.
- Ural M., Gönçüoğlu M.C., Tekin U.K. and Aslan M., 2013. Geology and geodynamic interpretation of the volcanic rocks of the Yüksekova Complex in Elazığ and surroundings. 19<sup>th</sup> Intern. Petrol. Natural Gas Congr., *Proceed.*, p. 317-319.
- Varol E., Bedi Y., Tekin U.K. and Uzunçimen S., 2011. Geochemical and petrological characteristics of Late Triassic basic volcanic rocks from the Kocali complex, SE Turkey: Implications for the Triassic evolution of southern Tethys. *Ofioliti*, 36: 101-115.
- Volker F., Altherr R., Jochum K.P. and McCulloch M.T., 1997. Quaternary volcanic activity of the southern Red Sea: new data and assessment of models on magma sources and Afar plume-lithosphere interaction. *Tectonophysics*, 278: 15-29.
- Walter M.J., 1998. Melting of garnet peridotite and the origin of komatite and depleted lithosphere. *J. Petrol.*, 39: 29-60.
- Winchester J.A. and Floyd P.A., 1977. Geochemical discrimination of different magma series and their differentiation products using immobile elements. *Chem. Geol.*, 20: 325-343.
- Wood D.A., Gibson I.L. and Thompson R.N., 1976. Elemental mobility during zeolite facies metamorphism of the Tertiary basalts of eastern Iceland. *Contrib. Mineral. Petrol.*, 55: 241-254.
- Workman R.K. and Hart S.R., 2005. Major and trace element composition of the depleted MORB mantle (DMM). *Earth Planet. Sci. Lett.*, 231: 53-72.
- Yılmaz Y., 1985. Geology of the Cilo Ophiolite; an ancient ensimatic island arc fragment on the Arabian Platform, SE Turkey. *Ofioliti*, 10: 457-487.
- Yılmaz Y., 1993. New evidence and model on the evolution of the Southeast Anatolia Orogen. *Geol. Soc. Am. Bull.*, 105: 251-271.
- Yılmaz A., Adamia S. and Yılmaz H., 2014. Comparisons of the suture zones along a geotraverse from the Scythian Platform to the Arabian Platform. *Geosci. Frontiers*, <http://dx.doi.org/10.1016/j.gsf.2013.10.004>